Bulk Prepolymerization of Styrene in the Presence of Polybutadiene: Determination of Grafting Efficiency by Size Exclusion Chromatography Combined with a New Extended Model

Natalia Casis, Diana A. Estenoz, Jorge R. Vega, Gregorio R. Meira

Instituto de Desarrollo Tecnológico para la Industria Química, Universidad Nacional del Litoral and Consejo Nacional de Investigaciones Científicas y Técnicas, Güemes 3450-3000 Santa Fe, Argentina

Received 10 August 2007; accepted 8 July 2008
DOI 10.1002/app.29137
Published online 30 October 2008 in Wiley InterScience (www.interscience.wiley.com).

ABSTRACT: The bulk prepolymerization of styrene in the presence of polybutadiene for the production of high-impact polystyrene is analyzed and compared with an equivalent solution reaction described by Estenoz et al. in 1999. The heterogeneous model reported by Casis et al. in 2006 is extended to predict the bivariate distributions of the graft copolymer topologies; each topology is characterized by the number of trifunctional branching points per molecule. The developed model assumes polymerization in two phases and requires the adjustment of a single kinetic parameter. Grafting efficiencies determined by solvent extraction/gravimetry are compared with determinations obtained by the deconvolution of size exclusion chromatograms of the total polymer. The chromatographic technique is fast and simple, but it requires a representative polymerization/fractionation model. © 2008 Wiley Periodicals, Inc. J Appl Polym Sci 111: 1508–1522, 2009

Key words: gel permeation chromatography (GPC); graft copolymers; modeling; polystyrene

INTRODUCTION

High-impact polystyrene (HIPS) is obtained through the polymerization of styrene (St) in the presence of polybutadiene (PB) and a chemical initiator. HIPS is a heterogeneous material with rubber particles dispersed in a vitreous polystyrene (PS) matrix. The rubber particles contain vitreous PS occlusions dispersed in a PB-rich phase. The occlusions increase the particle size and the material toughness[1] and are a mixture of low-molecular-weight PS and PS branches from the generated graft copolymer (GC). The mechanical properties depend on the molar mass of the continuous phase, the particle size distribution, and the particle volume fraction.[2–5]

HIPS is produced through a bulk free-radical process. The polymerization can be carried out in the bulk or in solution, and the reactors can be continuous, semicontinuous, or batch. The main reaction stages are prepolymerization and finishing. Prepolymerization is carried out under well-stirred conditions and in the presence of a chemical initiator. The bulk process is homogeneous up to about 2% conversion and thereafter is heterogeneous because of the thermodynamic incompatibility between PS and PB chains.[6–8] After the phase separation, free PS is produced in both phases, whereas GC is generated only in the PB-rich phase. Between the phase separation and phase inversion, the continuous phase is PB-rich. Thereafter, the PS-rich phase remains the continuous phase. The St grafting efficiency (i.e., the ratio of the mass of grafted St to the total mass of polymerized St) importantly affects the phase inversion. For high initial grafting efficiencies, early phase inversion takes place, with the generation of smaller rubber particles. For low initial grafting efficiencies (but similar stirring conditions), the phase inversion is delayed, with the generation of bigger particles and bigger particle occlusions.[9]

For several peroxide initiators, Ludwico and Rosen,[6] García et al.,[10] and Berlin et al.[11] determined the partition coefficients (defined as the ratio of their concentrations in the PS-rich and PB-rich phases). García et al. investigated the effects of the monomer conversion, initiator concentrations, and PS molecular weights on the partition of *tert*-butyl peroctoate (TBPO) in an St/PS/PB/initiator blend. TBPO was seen to preferably concentrate in the PS-rich phase, and this result was in accord with previous

Correspondence to: G. R. Meira (gmeira@santafe-conicet.gov.ar).
Contract grant sponsor: Consejo Nacional de Investigaciones Científicas y Técnicas.
Contract grant sponsor: Secretaria de Ciencia y Tecnologia.
Contract grant sponsor: Universidad Nacional del Litoral.

measurements by Ludwico and Rosen for *n*-butyl peroctoate (BPO). According to Berlin et al., the partition coefficients of peroxide initiators are all close to unity.

For a batch solution polymerization of St in the presence of PB at 70°C, Estenoz et al.[12] determined the global molecular macrostructure of the three polymeric components (free PS, residual PB, and GC). For batch and bulk polymerizations of St in the presence of PB, Casis et al.[13] developed a heterogeneous model that simulates the polymerization in two phases. It was validated through the analysis of two polymerizations, the St grafting efficiency having been determined by gravimetry and the molecular characteristics of the isolated polymeric components having been determined by size exclusion chromatography (SEC).[13] The gravimetric method provided values in excess of the St grafting efficiency because of the difficulty of quantitatively extracting all the free PS contained in the particle occlusions.[14]

By deconvolution of the ultraviolet (UV) chromatogram of the total polymer and with the help of a representative polymerization/SEC model, Estenoz et al.[15] developed a chromatographic technique for estimating the St grafting efficiency during a solution prepolymerization. It is based on simulating the molecular weight calibrations of each of the generated GC topologies, with each topology characterized by the number of trifunctional branches per molecule. Estenoz et al.[14] predicted that the GC generated during an HIPS process will exhibit an essentially constant composition independent of the molar mass or degree of branching. This is because the grafting reactions are proportional to the number of butadiene (Bd) units in each molecule; for this reason, longer PB chains are also more highly grafted. Thus, the different GC topologies [number of trifunctional grafting points per molecule (r) = 0, 1, 2, ...] are assumed to behave as branched homopolymers of a constant effective average composition.[15] Consider the SEC procedure for measuring branching distribution $G(r)$, where G is the mass of a branched homopolymer containing r long trifunctional branches. The raw measurements are the concentration chromatogram obtained from a differential refractometer, $A_{DR}(V_e)$, and the specific viscosity chromatogram, $A_{SV}(V_e)$, where V_e represents the elution volume. The calculation procedure is as follows:

1. Calculate the instantaneous intrinsic viscosity, $[\eta]_b(V_e)$, from the signal ratio, $A_{SV}(V_e)/A_{DR}(V_e)$.
2. Obtain $[\eta]_b(M)$, where M is the molar mass, by combining $[\eta]_b(V_e)$ with the universal calibration $\log\{[\eta]M\}$ versus V_e.
3. Calculate the variation with M of volumetric contraction parameter g':

$$g'(M) \equiv \frac{[\eta]_b(M_b)}{[\eta]_1(M_1)} = \frac{[\eta]_b(M_b)}{KM_1^{\alpha}} \leq 1 \quad (M = M_b = M_1) \tag{1}$$

where the subscripts b and l indicate branched and linear molecules, respectively, and K and α are the Mark–Houwink constants of the equivalent linear homologue.

4. Calculate contraction parameter g through

$$g(M) = [g'(M)]^{1/\varepsilon} (g \leq 1) \tag{2}$$

with[16]

$$g(M) \equiv \langle s^2(M_b)\rangle_b / \langle s^2(M_1)\rangle_1 \leq 1 \quad (M = M_b = M_1) \tag{3}$$

where ε is an empirical exponent and $\langle s^2 \rangle$ is the mean squared radius of gyration.

5. Obtain $r(M)$ from the Zimm–Stockmayer model:

$$g(M) = \left[\left(1 + \frac{r(M)}{7} \right)^{1/2} + \frac{4r(M)}{9\pi} \right]^{-1/2} \tag{4}$$

Finally, determine $G(r)$ by combining $r(M)$ with $G(M)$. From eqs. (1)–(4), under the assumption of a linear universal calibration of $\log\{[\eta]M(V_e)\} = A_2 - B_2V_e$, the following expression was obtained for the molar mass calibrations of the different branched topologies contained in the GC of HIPS:[14–17]

$$\log M(V_e, r) = \frac{A_2 - \log[g^{\varepsilon}(r)K_{BC}]}{\alpha_{BC} + 1} - \frac{B_2}{\alpha_{BC} + 1} V_e \quad (r = 1, 2, \ldots) \tag{5}$$

where K_{BC} and α_{BC} are the Mark–Houwink constants of a linear diblock copolymer of average composition identical to that of the GC. In the right-hand side of eq. (5), the first term and $B_2/(\alpha_{BC} + 1)$ are both constants. Thus, each of the GC topology calibrations are linear and parallel to one another.[14]

For a typical GC produced during an HIPS prepolymerization, Vega et al.[17] estimated the ε exponent of eqs. (2) and (5), obtaining $\varepsilon \cong 2$.

In this work, a bulk prepolymerization of St in the presence of PB is compared with an equivalent solution prepolymerization described by Estenoz et al.[12] The bulk process has been simulated with an extension of the heterogeneous mathematical model by Casis et al.[13] The new extended model calculates the molecular structure of each of the generated GC topologies, and it has been combined with an ideal SEC model for estimating the St grafting efficiency by deconvolution of the SEC chromatogram of the total HIPS.

EXPERIMENTAL

A bulk prepolymerization of St in the presence of PB at 70°C was carried out. The recipe and reaction

TABLE I
Bulk and Solution Prepolymerizations: Recipes and Experimental Conditions

	Bulk process	Solution process[a]
Monomer concentration: $[St]^0$	7.67 mol/L	2.93 mol/L
Concentration of Bd repeating units of PB: $[B^*]^0$	0.333 mol/L[b]	0.127 mol/L[c]
Concentration of the initiator (TBPO): $[I_2]^0$	0.00490 mol/L	0.00187 mol/L
Concentration of toluene	0.94 mol/L	6.15 mol/L
Temperature	70°C[d]	70°C[d]
Stirring rate	125 rpm	125 rpm
Final time	475 min	960 min
Final conversion	17.70%	17.60%

[a] Taken from Estenoz et al.[12]
[b] $M_{n,PB} = 121{,}000$; $M_{w,PB} = 245{,}000$.
[c] $M_{n,PB} = 115{,}385$; $M_{w,PB} = 221{,}154$.
[d] Includes a heating period of 1°C/min from 25°C.

conditions (Table I) are compared with the values of an equivalent solution polymerization described by Estenoz et al.[12] Consider the solution polymerization.[12] First, PB was dissolved in the monomer at room temperature for 24 h, and the solution was loaded into a three-necked, 1-L glass reactor.[12] Then, the temperature was raised to 70°C, the monomer and initiator were added, and the remaining solvent was incorporated to complete 500 mL. Reaction samples were taken at 8, 12, and 16 h. The initial rubber concentration was relatively low (ca. 2.3 wt % with respect to the pure monomer) to ensure homogeneity. The monomer conversion and grafting efficiencies were determined by solvent extraction/gravimetry.[12] The measurements and homogeneous model predictions are reproduced in Figure 1.

Equivalent bulk polymerization

The bulk prepolymerization was carried out in a 2-L stainless steel reactor. The applied temperature profile was controlled by simultaneous circulation of hot oil through an external jacket and cold water through an internal serpentine. As shown in Table I, except for the solvent, the relative amounts of the initial monomer, PB, and initiator coincided with their corresponding solution polymerization values. The molecular weight distribution (MWD) of the initial PB is not presented here for reasons of space, but its average molecular weights were close to those of the equivalent solution process (Table I). The St monomer (technical-grade; Petrobras Energía S.A., Puerto San Martin, Argentina) was vacuum-distilled. The toluene solvent (E. M. Science, Darmstadt, Germany) and the TBPO initiator (Akzo Chemicals, Itupeba, Brazil) were used as received.

The prepolymerization was as follows. First, the rubber was dissolved in the monomer at room temperature for 12 h in a glass flask, and toluene was added to complete 1 L. The resulting solution (ca. 10 vol % solvent) was loaded into the reactor, N_2 was bubbled for 10 min to eliminate dissolved oxygen, and the temperature was raised at 1°C/min from room temperature to 70°C. The prepolymerization was started with the incorporation of the initiator. During the reaction, 20-mL samples were taken at conversions of around 9, 13, and 18% (Table II). Because of the relatively low temperatures and conversions, crosslinking was not observed in the final sample.

The monomer conversion and grafting efficiencies were determined with the following solvent extraction/gravimetry technique. First, the polymer was isolated from the low-molar-mass material by precipitation in 200 mL of methanol, decantation, and vacuum drying until a constant weight was obtained. The conversion was calculated after subtraction of the original PB mass. The St grafting efficiency was determined after extraction of the free PS from the total polymer with methyl ethyl ketone. The PB grafting efficiency (i.e., the mass of grafted PB divided by the initial PB mass) was determined through a second solvent extraction procedure applied to the insoluble PB/GC mixture. It involved extracting the GC from the unreacted PB by dissolution of the former into petroleum ether (Fisher Scientific, Fair Lawn, NJ). The mass of grafted PB was estimated from the difference between the initial and residual PB masses.

As later explained in detail, the St grafting efficiency was also determined through an extension of the SEC model technique described by Estenoz et al.[15] The measurements are the UV chromatograms of the total polymers (Fig. 2). The size exclusion chromatograph was a Waters Breeze (Milford, MA) fitted with a full set of six μ-Styragel columns and a UV sensor at 254 nm (Waters 440). The injected samples were obtained by precipitation of the total polymer from the reaction mixture, drying, and redissolution of the solid.

The average molecular weights of the isolated HIPS components (free PS, GC, and unreacted PB) were also determined by SEC. To this effect, the chromatograph was fitted with a Viscotek (Porter, TX), 200 detector (containing an online viscometer in parallel with a differential refractometer) and the aforementioned set of μ-Styragel columns. The carrier solvent was tetrahydrofuran at 1 mL/min. The injection volume was 0.25 mL at a nominal polymer concentration of 1.0 mg/mL. The MWDs were obtained from measurements of the intrinsic viscosity and a universal calibration determined from a set of PS standards.

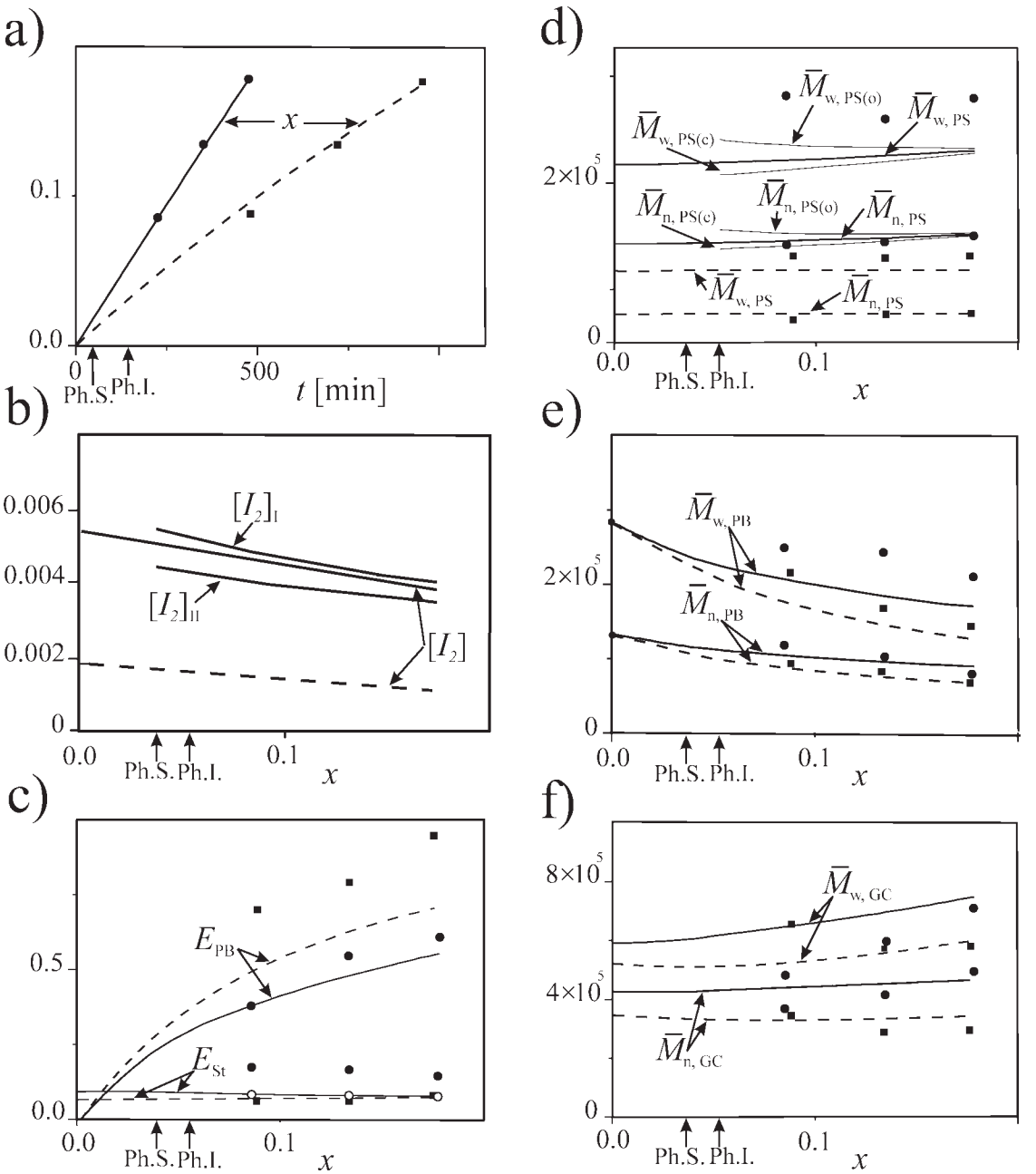

Figure 1 Bulk prepolymerization: (●,○) measurements and (—) predictions. Also presented are (■, - - -) the results from Estenoz et al.,[12] which correspond to an equivalent solution prepolymerization. (a) Time evolution of monomer conversion. (b) Initiator concentration versus conversion. (c) St and PB grafting efficiencies versus conversion. In the bulk reaction, E_{St} was measured by (●) solvent extraction/gravimetry and (○) the SEC model. (d) Average molecular weights versus the conversion of the global free PS, free PS accumulated in the continuous phase [PS(c)], and free PS accumulated in the occlusion region [PS(o)]. (e,f) Average molecular weights versus the conversion of the GC and residual PB. For the bulk reaction, Ph.S. and Ph.I. indicate the predicted conversions at the phase-separation and phase-inversion points, respectively.

The final measurements are presented in Table II and in Figures 1–3. Compared with the solution reaction results, the bulk prepolymerization exhibited higher reaction rates [Fig. 1(a)]. This was a result of a more pronounced gel effect and the increased reagent concentrations. For the bulk reaction, the St grafting efficiencies determined by solvent extraction/gravimetry were considerably higher than those obtained by the SEC model [Fig. 1(c) and Table II]. These differences possibly arose from errors in excess in the solvent extraction technique measurements caused by undissolved free PS that contaminated the insoluble PB/GC. Finally, the determinations of the St grafting efficiencies of the bulk reaction samples via the SEC model almost coincided with the solvent extraction/gravimetry

TABLE II
Bulk Prepolymerization: Measurements and Theoretical Predictions

		$t = 225$ min		$t = 350$ min		$t = 475$ min	
		Measured	Model	Measured	Model	Measured	Model
x (%)		8.53	9.42	13.40	13.17	17.80	17.67
G_{PS} (g)		61.5	69.81	87.35	98.50	119.52	133.42
G_{PB} (g)		8.87	10.32	7.66	8.58	4.87	7.32
G_{GC} (g)		13.34	12.99	13.81	16.09	14.74	18.19
E_{St} (%)		18.1[a]	7.09	16.9[a]	6.36	15.2[a]	5.34
		8.43[b]		7.74[b]		6.67[b]	
E_{PB} (%)		50.67[a]	42.6	57.4[a]	52.3	72.9[a]	59.3
PS	$M_{n,PS}$ (g/mol)	134,000	139,300	137,000	139,900	142,000	143,400
	$M_{w,PS}/M_{n,PS}$	2.08	1.63	1.875	1.64	1.82	1.61
PB	$M_{n,PB}$ (g/mol)	115,000	103,600	107,000	99,400	82,200	95,300
	$M_{w,PB}/M_{n,PB}$	2.17	2.12	2.44	1.86	1.82	1.88
GC	$M_{n,GC}$ (g/mol)	370,000	452,000	416,000	466,100	516,000	480,000
	$M_{w,GC}/M_{n,GC}$	1.3	1.42	1.44	1.5	1.51	1.56
$\bar{p}_S$ (%)		40.00	41.01	43.00	41.56	47.00	41.38
Branches/molecule		—	1.49	—	1.81	—	2.08

[a] By solvent extraction/gravimetry.
[b] By the SEC model.

measurements of the solution polymerization samples [Fig. 1(c)]. (In the solution polymerization samples, complete dissolution of the free PS from the insoluble GC/PB was possible, and so the mentioned errors were not generated in excess.) Because of the increased gel effect, the molecular weights of the free PS and GC were higher in the bulk reaction [Fig. 1(d–f)]. Also, the free PS of the bulk polymerization samples exhibited a higher polydispersity. In the bulk reaction, the molecular weights of the residual PB were also higher because of the lower PB grafting efficiency. These lower PB grafting efficiencies for similar St grafting efficiencies according to the SEC model were a result of the longer PS branches of the bulk process GC.

Figure 3 presents (in a continuous trace) the measured MWDs of the total polymer and its three polymeric constituents. To provide an easier comparison with the theoretical predictions, the areas under the measured distributions are shown to be proportional to the mass fractions, as predicted by the polymerization model. As expected, the GC exhibited higher molecular weights. The MWD of the total polymer (in a broader continuous trace) was close to the distribution obtained when the MWDs of its individual components were added together (in a finer continuous trace). At the final conversion, the free PS was the main polymeric component, whereas the GC was most abundant at the high-molecular-weight end.

EXTENDED POLYMERIZATION MODEL

The heterogeneous HIPS model by Casis et al.[13] was extended to calculate the detailed molecular structure of the evolving GC topologies. The kinetic mechanism (Table III) was applied to the PS-rich and PB-rich phases. The GC topologies were classified according to the number of trifunctional grafting points per molecule ($r = 1, 2, \ldots$). A generic GC species is represented by $P_{(r)}(s,b)$, where r is the topology and s and b are the number of St and Bd repetitive units, respectively. In agreement with Casis et al.,[13] the phase-separation point was determined through a ternary equilibrium diagram (Fig. 4) for the St/PS/PB blend (i.e., neglecting the presence of GC), and the phase inversion was assumed to occur under the condition of equal phase volumes. Between the phase separation and the phase inversion, the free PS was produced in both phases, but it accumulated only in the PS-rich phase. Before the phase inversion, the PS-rich phase was the dispersed phase. After the phase inversion, the PS-rich phase was subdivided into two regions: a continuous region indicated by subscript c and a particle occlusion region indicated by subscript o.

The polymerization model is presented in Appendix A. The computer model was based on eqs. (A.1)–(A.7) and (A.14)–(A.27), and the following were calculated: (1) the conversion and phase compositions; (2) the univariate MWDs of the free PS and unreacted PB [$G_{PS}(s)$ and $G_{PB}(b)$, respectively]; (3) the bivariate weight chain length distributions (WCLDs) of each GC topology [$G_{GC_{(r)}}(s,b)$] and of the total GC [$G_{GC}(s,b)$]; and (4) the number-average number of PS branches per GC molecule. Finally, the univariate MWDs of the GC topologies and total GC [$G_{GC_{(r)}}(M)$ and $G_{GC}(M)$, respectively] were calculated from their corresponding bivariate WCLDs.

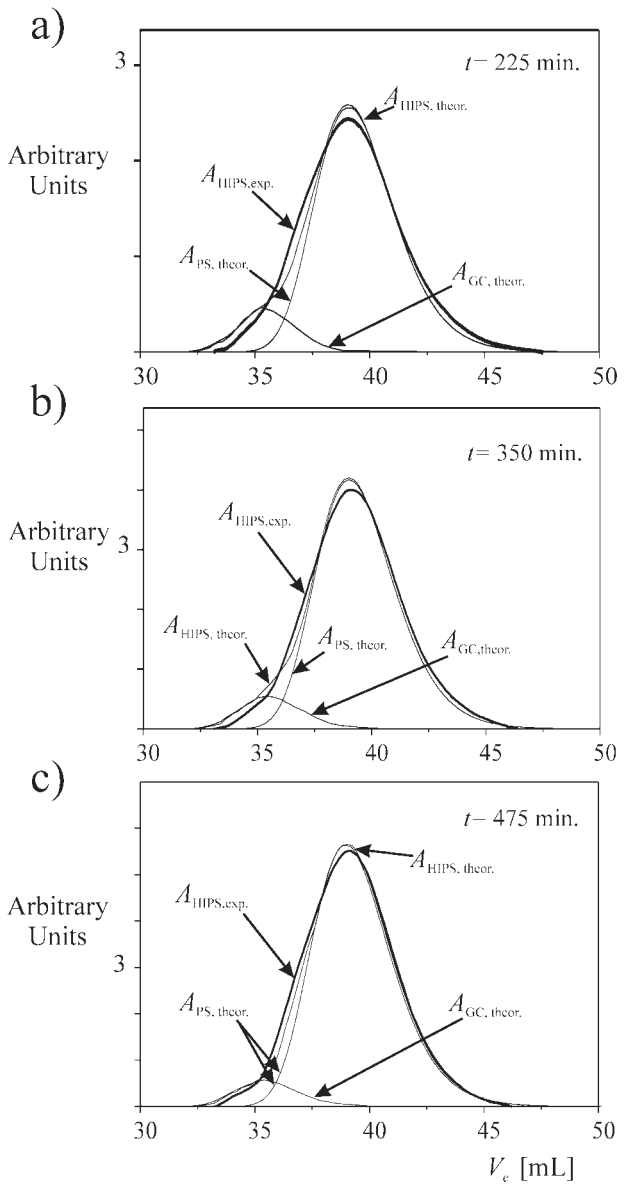

Figure 2 Bulk prepolymerization: chromatographic determination of the St grafting efficiencies for the samples taken at 225, 350, and 475 min. The measured UV chromatograms of the total HIPS [$A_{HIPS,exp.}(V_e)$] are compared with the model predictions [$A_{HIPS,theor.}(V_e)$]. In turn, $A_{HIPS,theor.}(V_e)$ receives contributions from the free PS [$A_{PS,theor.}(V_e)$] and from the PS branches contained in the GC [$A_{GC,theor.}(V_e)$].

The model parameters are presented in Table IV. They coincide with those of Casis et al.,[13] except for (1) the initiator partition coefficient, because the initiator employed in this work (TBPO) differs from that of Casis et al.[13] (BPO), and (2) the initiation ratio k_{i1}/k_{i2} [where k_{i1} is the rate constant of initiation to the monomer and k_{i2} is the rate constant of initiation to the rubber, as shown in eqs. (7) and (8) of Table III]. For the initiator partition coefficient, a linear relationship was adjusted to measurements by García et al.[10] (last row of Table IV). The kinetic ratio k_{i1}/k_{i2} was the adjustable parameter because of its direct influence on the St grafting efficiency and because k_{i2} is the least known parameter of Table IV. As explained later in more detail, the initial value of k_{i1}/k_{i2} was initially taken from Casis et al.,[13] but it was readjusted to the chromatographic measurements of Figure 2 (Table IV).

The differential equations [eqs. (A.1)–(A.3)] were solved by standard numerical techniques appropriate for stiff differential equations. These equations were jointly solved with the set of algebraic equations [eqs. (A.4)–(A.7) and (A.14)–(A.19)] by means of standard nonlinear routines. Equations (A.21)–(A.27) were solved by finite difference methods: lumping together many molecular species at fixed chain length intervals. Thus, 1000 hypothetical chain lengths were adopted for the PS and PB homopolymers, whereas 150 × 150 hypothetical chain lengths were adopted for the bivariate distribution of the GC. The computer program was written in Fortran 95, and a typical run involved 2 min in a Pentium III personal computer.

For the recipe and experimental conditions of the investigated bulk process (Table I), consider the model predictions of Table II and Figure 1. In Figure 1(a,c–f), a reasonable agreement between the measurements and predictions can be observed. After the phase separation, the subscripts I and II indicate the PS-rich and PB-rich phases, respectively. According to the model, the phase inversion (estimated under the condition of equal volumes) occurred at 6% conversion. This early inversion was a result of the low initial rubber content (2.3 wt %) instead of the more common values of 6–8 wt %. Figure 1(b) presents the predicted evolution of the global

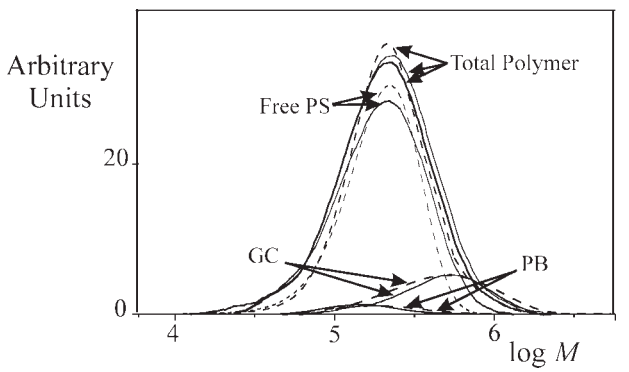

Figure 3 Bulk prepolymerization: MWDs of the final sample at $t = 475$ min. The measured distributions of the total polymer and its three polymeric components (in continuous traces) are compared with the model predictions (in dashed traces). For the total polymer, the direct measurement is represented by a broader continuous trace, whereas the thinner continuous trace was obtained by the addition of the MWD measurements of the free PS, residual PB, and GC.

TABLE III
Kinetic Mechanism (Applied to Both Phases)

Chemical initiation:

$$I_2 \xrightarrow{k_d} 2I^{\cdot} \quad (6)$$

$$I^{\cdot} + St \xrightarrow{k_{i1}} S_1^{\cdot} \quad (7)$$

$$I^{\cdot} + P_{(r)}(s,b) \xrightarrow{k_i 2} P_{0(r)}^{\cdot}(s,b) \quad (8)$$

Thermal initiation:

$$3St \xrightarrow{k_{i3}} 2S_i \quad (9)$$

Propagation:

$$S_n^{\cdot} + St \xrightarrow{k_p} S_{n+1}^{\cdot} \quad (10)$$

$$P_{0_{(r)}}^{\cdot}(s,b) + St \xrightarrow{k_{p0}} P_{1(r)}^{\cdot}(s,b) \quad (11)$$

$$P_{n_{(r)}}^{\cdot}(s,b) + St \xrightarrow{k'_p} P_{n+1(r)}^{\cdot}(s,b) \quad (12)$$

Transfer to the monomer:

$$S_n^{\cdot} + St \xrightarrow{k_{fm}} S_n + S_1^{\cdot} \quad (13)$$

$$P_{m(r-1)}^{\cdot}(s-m,b) + St \xrightarrow{k_{fm}} P_{(r)}(s,b) + S_1^{\cdot} \quad (14)$$

$$P_{0_{(r)}}^{\cdot}(s,b) + St \xrightarrow{k'_{fm}} P_{(r)}(s,b) + S_1^{\cdot} \quad (15)$$

Transfer to PB or the copolymer:

$$S_n^{\cdot} + P_{(r)}(s,b) \xrightarrow{k_{fg}} S_n + P_{0_{(r)}}^{\cdot}(s,b) \quad (16)$$

$$P_{m(r-1)}^{\cdot}(s-m,b) + P_{(r_1)}(s_1,b_1) \xrightarrow{k_{fg}} P_{(r)}(s,b) + P_{0_{(r_1)}}^{\cdot}(s_1,b_1) \quad (17)$$

Termination by combination:

$$S_n^{\cdot} + S_m^{\cdot} \xrightarrow{k_{tc}} S_{n+m} \quad (18)$$

$$P_{m-n_{(r-1)}}^{\cdot}(s-m,b) + S_m^{\cdot} \xrightarrow{k_{tc}} P_{(r)}(s,b) \quad (19)$$

$$P_{m-n_{(r-r_1-1)}}^{\cdot}(s-s_1-m,b-b_1) + P_{n_{(r_1-1)}}^{\cdot}(s_1,b_1) \xrightarrow{k_{tc}} P_{(r)}(s,b) \quad r > (r_1-1) \quad (20)$$

$$P_{0_{(r-r_1-1)}}^{\cdot}(s-s_1-n,b-b_1) + P_{n_{(r_1)}}^{\cdot}(s_1,b_1) \xrightarrow{k''_{tc}} P_{(r)}(s,b) \quad r > (r_1-1) \quad (21)$$

$$P_{0_{(r-1)}}^{\cdot}(s-n,b) + S_n^{\cdot} \xrightarrow{k''_{tc}} P_{(r)}(s,b) \quad (22)$$

initiator concentration ($[I_2]$). The partition coefficients of TBPO (K_{I_2} in Table IV) determine a slight preference for the PS-rich phase. Consider the grafting efficiency predictions of Figure 1(c). According to the model, the PB grafting efficiencies are lower in the bulk process (because of the lower initiator concentration in the rubber phase), whereas the St grafting efficiencies are almost coincident in both processes. The molecular weights of the free PS and GC slowly increase because of the increasing gel effect [Fig. 1(d,f)]. Figure 1(d) presents the average molecular weights of the global free PS (in a thicker trace) and its fractions (after the phase inversion). The weight-average and number-average molecular weights of the free PS that accumulated in the particle occlusions ($M_{w,PS(o)}$ and $M_{n,PS(o)}$) are higher than those of the continuous region ($M_{w,PS(c)}$ and $M_{n,PS(c)}$). This is caused by a higher gel effect in the PB-rich phase, which is combined with the preferential partition of the initiator into the PS-rich phase. In comparison with the solution process, the polydispersity of the global free PS generated in the bulk polymerization is larger than that of the solution process. The reason for this is the different average molar masses of the free PS fractions produced after the phase inversion in the two PS-rich regions: the continuous region and the particle occlusion region.

Figure 5(a) shows the model predictions for the MWDs of the final GC and its main topologies. As expected, the higher topologies also exhibit higher molecular weights. The single-branched topology remains the most abundant, despite the incipient grafting-over grafting process. In Figure 5(b), the areas under the MWDs of the different GC

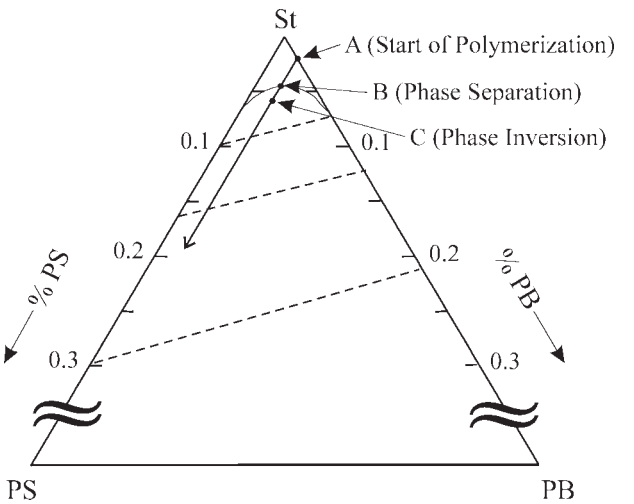

Figure 4 Phase diagram of the St–PB–PS system, showing the reaction path. Point A represents the start of the polymerization, point B represents the phase separation, and point C represents the phase inversion. Reprinted with permission from Casis et al.[13].

TABLE IV
Polymerization Model Parameters

Parameter	Expression	Value at 70°C
f	—	0.5[a]
k_d (s^{-1})	$9.1 \times 10^{13} e^{-29508/RT}$ a	1.443×10^{-5} a
$k_{tc} = k'_{tc} = k''_{tc}$ [L/(mol s)]	$1.7 \times 10^{9}\ e^{-(1667.3/RT)-2(C_1\psi_i + C_2\psi_i^2 + C_3\psi_i^3)}$ a,b	$1.473 \times 10^{8}\ e^{-2(0.84\psi_i+3.52\psi_i^2-3.37\psi_i^3)}$ a,b
$k_p = k_{i1} = k_{i3}$ [L/(mol s)]	$1.0 \times 10^{7} e^{-7067/RT}$ a	314.2[a]
k_{i0} [L^2/(mol^2 s)]	$1.1 \times 10^{5} e^{-27340/RT}$ a	4.18×10^{-13} a
$k_{fm} = k'_{fm}$ [L/(mol s)]	$4.414 \times 10^{14} e^{-13532/T}$ a	3.244×10^{-3} a
k_{i1}/k_{i2}	—	1.3 (initial value)[a]
		1.1[c]
k_{fs} [L/(mol s)]	$1.0487 \times 10^{11} e^{-9424.2/T}$ a	1.224×10^{-1} a
K_{I_2}	$0.80541 + 0.2192x$[c]	—

[a] Adopted from Casis et al.[13]
[b] ψ_i = polymer volume fraction in phase i; $C_1 = 2.57 - 0.00505T$; $C_2 = 9.56 - 0.0176T$; $C_3 = -3.03 + 0.00785T$.
[c] Adjusted in this work.

topologies of Figure 5(a) are represented by discrete bars in a distribution of chain branching.

CHROMATOGRAPHIC DETERMINATION OF THE ST GRAFTING EFFICIENCY

Consider the estimation of the St grafting efficiency from the UV chromatograms of the total HIPS (Fig. 2). The method is based on the following assumptions:[17] (1) at 256 nm, the UV sensor sees the phenyl groups of the PS chains but not the Bd repeating units, and (2) the molar masses of the GC are higher than those of the free PS, and for this reason it is possible to deconvolute the total UV chromatogram into the chromatograms of the free PS and the grafted PS branches.

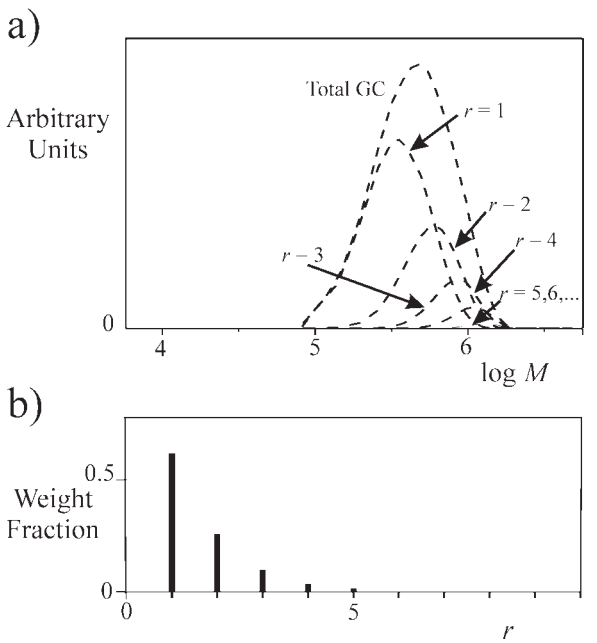

Figure 5 Bulk prepolymerization: model predictions for the GC of the final sample at t = 475 min. (a) MWDs of the total GC and main GC topologies. (b) Distribution of chain branching.

Then, the St grafting efficiency is given by the ratio of the area under the grafted PS branches to the area under the total UV chromatogram.[17]

The SEC model for simulating the UV chromatograms is presented in Appendix B. It was solved together with the polymerization model of Appendix A. The SEC model assumes ideal fractionation according to the hydrodynamic volume, and the input data include the monomer conversion, the MWD of the free PS [$G_{PS}(M_{PS})$], the MWDs of each of the r topologies [$G_{GC_{(r)}}(M)$], and the global average mass fraction of St in the GC [$\overline{p}_S$]. The SEC model parameters are presented in Table V. They include the direct and universal calibrations obtained with PS standards, the Mark–Houwink parameters of an equivalent linear St–Bd diblock copolymer of an average molar mass and composition similar to that of the analyzed GC (K_{BC} and α_{BC}), and the branching exponent ε.[17]

As mentioned before, the initiation ratio k_{i1}/k_{i2} was readjusted to fit the UV chromatograms of the total HIPS presented in Figure 2. The following iterative procedure was applied: (1) adopt an initial k_{i1}/k_{i2} value of 1.3 (as suggested by Casis et al.[13]) and simulate the polymerization model to obtain (at the measured conversions) the MWD of the free PS [$G_{PS}(M_{PS})$], the MWDs of each of the GC topologies [$G_{GC_{(r)}}(M)$], and their (common) average composition [$\overline{p}_S$]; (2) use eqs. (A.29) and (A.30) to calculate the UV

TABLE V
SEC Model Parameters in Tetrahydrofuran at 25°C

PS calibration	$\log M_{PS} = A_1 - B_1 V_e$ with $A_1 = 11.265$ and $B_1 = 0.1516$
Universal calibration	$\log\{[\eta]M\} = A_2 - B_2 V_e$ with $A_2 = 15.3926$ and $B_2 = 0.2595$
Mark–Houwink constants of a linear homologue of the GC	$K_{BC} = 3.2 \times 10^{-4}$ dL/g $\alpha_{BC} = 0.693$
Exponent of eq. (2)	$\varepsilon = 2$

chromatograms of the free PS and each GC topology; (3) calculate the UV chromatogram of the total GC by the addition of the individual chromatograms and then the UV chromatogram of the total HIPS through eq. (A.31); (4) compare the predicted chromatograms of the total HIPS with the measurements, readjust k_{i1}/k_{i2}, and iterate until an acceptable fit is achieved; and (5) with the readjusted polymerization model, predict the masses of free and grafted PS chains (G_{PS} and G_{GS}, respectively) and estimate the St grafting efficiency through $E_{St} = G_{GS}/(G_{GS} + G_{PS})$. Finally, note that G_{GS} and $G_{GS} + G_{PS}$ are also the areas under the simulated UV chromatograms of the GC and total HIPS, respectively. The iterative procedure yielded $k_{i1}/k_{i2} = 1.1$ (Table IV), and the St grafting efficiencies are listed in Table II and Figure 1(c).

CONCLUSIONS

A bulk prepolymerization of St in the presence of PB was compared with an equivalent solution prepolymerization. The increased gel effect of the bulk process increased the rate of polymerization and average molar masses of the free PS and grafted PS chains (which almost doubled their equivalent solution reaction values).

A new heterogeneous polymerization model was developed that calculates the polymerization in two phases and predicts the detailed molecular structure of the generated GC topologies. The polymerization model was combined with an ideal SEC model for estimating the St grafting efficiency. The technique is fast and efficient during the vital prepolymerization stage, and it involves the adjustment of a single polymerization model parameter. The SEC analysis is reasonable because all of the polymer remains completely soluble at the relatively low temperatures and conversions of the prepolymerization stage. Of course, the difficulty of the chromatographic technique is the development of a representative polymerization/SEC model. However, such an effort seems justified in industry, for which a quick and accurate estimation of the St grafting efficiency during prepolymerization is essential for adequate control of the particle morphology.

APPENDIX A: POLYMERIZATION MODEL

Call $S^{\cdot}_n$ (with $n = 1, 2, 3, \ldots$), $P^{\cdot}_{0(r)}(s,b)$ (with $r, s = 0, 1, 2, \ldots$ and $b = 1, 2, 3, \ldots$), and $P^{\cdot}_{n(r)}(s,b)_{(r)}$ (with $n = 2, 3, \ldots$; $r, s = 0, 1, 2, \ldots$; and $b = 1, 2, 3, \ldots$) a generic polystyryl radical, a generic primary rubber radical, and a generic GC radical, respectively. Their global concentrations are obtained through the following summations: $[S^{\cdot}] = \sum_n [S^{\cdot}_n]$, $[P^{\cdot}_0] = \sum_r \sum_s \sum_b [P^{\cdot}_{0_{(r)}}(s,b)]$, and $[P^{\cdot}] = \sum_r \sum_s \sum_b \sum_n [P^{\cdot}_{n_{(r)}}(s,b)]$. Call V the total reaction volume, and call V_I and V_{II} the volumes of the PS-rich and PB-rich phases, respectively. Also, call B* any ungrafted Bd unit contained either in the GC or in the initial PB. The following material balances have been derived from the kinetic mechanism of Table III:

$$\frac{d}{dt}[I_2]V = -k_d([I_2]_I V_I + [I_2]_{II} V_{II}) \quad i = I, II \tag{A.1}$$

$$\frac{d}{dt}[St]V = -k_p\{[St]_I([S^{\cdot}]_I + [P^{\cdot}]_I)V_I + [St]_{II}([S^{\cdot}]_{II} + [P^{\cdot}]_{II})V_{II}\} = -R_p V \quad i = I, II \tag{A.2}$$

$$\frac{d}{dt}[B^*]V = -\{k_{i2}[I^{\cdot}]_I + k_{fg}([P^{\cdot}]_I + [S^{\cdot}]_I)\}[B^*]_I V_I + (k'_{fm}[St]_I[P^{\cdot}_0]_I V_I) - \{k_{i2}[I^{\cdot}]_{II} + k_{fg}([P^{\cdot}]_{II} + [S^{\cdot}]_{II})\}[B^*]_{II} V_{II} + k'_{fm}[St]_{II}[P^{\cdot}_0]_{II} V_{II} \quad i = I, II \tag{A.3}$$

$$\frac{d}{dt}([I^{\cdot}]_i V_i) = (2fk_d[I_2]_i - k_{i1}[St]_i[I^{\cdot}]_i - k_{i2}[I^{\cdot}]_i[B^*]_i) \times V_i \cong 0 \quad i = I, II \tag{A.4}$$

$$\frac{d}{dt}([S^{\cdot}]_i V_i) = \{k_{i1}[St]_i[I^{\cdot}]_i + 2k_{i0}[St]_i^3 + k'_{fm}[St]_i[P^{\cdot}_0]_i + k_{fm}[St]_i[P^{\cdot}]_i - k_{fg}[B^*]_i[S^{\cdot}]_i - k''_{tc}[P^{\cdot}_0]_i[S^{\cdot}]_i - k_{tc}([S^{\cdot}]_i + [P^{\cdot}]_i)[S^{\cdot}]_i\} \quad V_i \cong 0 \quad i = I, II \tag{A.5}$$

$$\frac{d}{dt}([P^{\cdot}]_i V_i) = k_{i3}[St]_i[P^{\cdot}_0]_i V_i - \{k_{fm}[St]_i + k'_{fg}[B^*]_i + k_{tc}([S^{\cdot}]_i + [P^{\cdot}]_i) + k''_{tc}[P^{\cdot}_0]_i\}[P^{\cdot}]_i V_i \cong 0 \quad i = I, II \tag{A.6}$$

$$\frac{d}{dt}([P^{\cdot}_0]_i V_i) = \{(k_{i2}[I^{\cdot}]_i + k_{fg}([S^{\cdot}]_i + [P^{\cdot}]_i))[B^*]_i - (k_{i3}[St]_i + k'_{fm}[St]_i + k'_{tc}[P^{\cdot}_0]_i + k''_{tc}([S^{\cdot}]_i + [P^{\cdot}]_i))[P^{\cdot}_0]_i\} \quad V_i \cong 0 \quad i = I, II \tag{A.7}$$

where $I^{\cdot}$ is a primary initiator radical, $P^{\cdot}$ is a generic GC radical with a growing polystyryl chain, $S^{\cdot}$ is a primary St radical, $P^{\cdot}_0$ is a generic primary rubber radical, R_p is the global rate of St consumption, f is the initiator efficiency, k_{i3} is the rate constant of thermal monomer initiation, k_{fg} is the rate constant of chain transfer to the rubber, k_{tc} and k_{tc}'' are the rate constants of termination by recombination, k_{fm} and k_{fm}' are the rate constants of chain transfer to the monomer, k_d is the initiator decomposition rate constant, and k_p is the propagation rate constant. The integration of eqs. (A.1)–(A.7) provides the global concentrations of reagents and free radicals in each

of the phases. The mass balances of all the different GC free radicals of topology $r = 1, 2, \ldots$ contained in each phase, together with the pseudo-steady-state assumption, yield the following:

$$\frac{d}{dt}([\mathrm{P}^{\cdot}_{0_{(r)}}(s,b)]_i V_i) = \{(k_{i2}[\mathrm{I}^{\cdot}]_i + k_{fg}([\mathrm{S}^{\cdot}]_i + [\mathrm{P}^{\cdot}]_i))[\mathrm{B}^{*}_{(r)}(s,b)]_i - (k_{i3}[\mathrm{St}]_i + k'_{fm}[\mathrm{St}]_i + k'_{tc}[\mathrm{P}^{\cdot}_0]_i + k''_{tc}([\mathrm{S}^{\cdot}]_i + [\mathrm{P}^{\cdot}]_i)) \times [\mathrm{P}^{\cdot}_{0_{(r)}}(s,b)]_i\} V_i \cong 0$$
$$r,s = 0,1,2,\ldots;\ b = 1,2,3,\ldots \quad i = \mathrm{I},\mathrm{II} \qquad (A.8)$$

$$\frac{d}{dt}\{[\mathrm{P}^{\cdot}_{1_{(r)}}(s,b)]_i V_i\} = k_{i3}[\mathrm{St}]_i[\mathrm{P}^{\cdot}_{0_{(r)}}(s,b)]_i V_i - (k_p + k_{fm}) \times [\mathrm{St}]_i[\mathrm{P}^{\cdot}_{1_{(r)}}(s,b)]_i V_i - \{k_{fg}[\mathrm{B}^{*}]_i + k''_{tc}[\mathrm{P}^{\cdot}_0]_i + k_{tc}([\mathrm{S}^{\cdot}]_i + [\mathrm{P}^{\cdot}]_i)\} [\mathrm{P}^{\cdot}_{1_{(r)}}(s,b)]_i V_i \cong 0$$
$$r,s = 0,1,2,\ldots;\ b = 1,2,3,\ldots \quad i = \mathrm{I},\mathrm{II} \qquad (A.9)$$

$$\frac{d}{dt}\{[\mathrm{P}^{\cdot}_{n_{(r)}}(s,b)]_i V_i\} = k_p[\mathrm{St}]_i[\mathrm{P}^{\cdot}_{n-1_{(r)}}(s,b)]_i V_i - (k_p + k_{fm})[\mathrm{St}]_i[\mathrm{P}^{\cdot}_{n_{(r)}}(s,b)]_i V_i - \{k_{fg}[\mathrm{B}^{*}]_i + k''_{tc}[\mathrm{P}^{\cdot}_0]_i + k_{tc}([\mathrm{S}^{\cdot}]_i + [\mathrm{P}^{\cdot}]_i)\}[\mathrm{P}^{\cdot}_{n_{(r)}}(s,b)]_i V_i \cong 0$$
$$n = 2,3,\ldots \quad r,s = 0,1,2,\ldots;\ b = 1,2,3,\ldots \quad i = \mathrm{I},\mathrm{II} \qquad (A.10)$$

where $\mathrm{B}^{*}_{(r)}(s,b)$ is any nongrafted Bd unit of $\mathrm{P}_{(r)}(s,b)$.

Comparing eqs. (A.7) and (A.8), we find

$$\frac{[\mathrm{P}^{\cdot}_{0_{(r)}}(s,b)]_i}{[\mathrm{P}^{\cdot}_0]_i} = \frac{[\mathrm{B}^{*}_{(r)}(s,b)]_i}{[\mathrm{B}^{*}]_i},$$
$$r,s = 0,1,2\ldots;\ b = 1,2,3\ldots;\ i = \mathrm{I},\mathrm{II} \qquad (A.11)$$

The bivariate number chain length distribution (NCLD) of each GC topology is obtained from[12]

$$\frac{d}{dt}\{[\mathrm{P}_{(r)}(s,b)]V\} = \sum_i \{T_{1_i} + T_{2_i} + T_{3_i} + T_{4_i}\}$$
$$r,s,b = 1,2,3,\ldots; \quad i = \mathrm{I},\mathrm{II} \qquad (A.12a)$$

with

$$T_{1_i} = [\mathrm{B}^{*}_{(r)}(s,b)]_i\{k_{i2}[\mathrm{I}^{\cdot}]_i + k_{fg}([\mathrm{S}^{\cdot}]_i + [\mathrm{P}^{\cdot}]_i)\}V_i \quad i = \mathrm{I},\mathrm{II} \qquad (A.12b)$$

$$T_{2_i} = k_{fm}[\mathrm{St}]_i \sum_{m=1}^{s}[\mathrm{P}^{\cdot}_{m(r-1)}(s-m,b)]_i V_i + k_{tc}\sum_{m=2}^{s}\sum_{n=1}^{m-1}[\mathrm{P}^{\cdot}_{n(r-1)}(s-m,b)]_i[\mathrm{S}^{\cdot}_{m-n}]_i V_i + k''_{tc}\sum_{m=1}^{s}[\mathrm{P}^{\cdot}_{0(r-1)}(s-m,b)]_i[\mathrm{S}^{\cdot}_{m}]_i V_i \quad i = \mathrm{I},\mathrm{II} \qquad (A.12c)$$

$$T_{3_i} = \frac{k_{tc}}{2}\sum_{b_1=1}^{b-1}\sum_{s_1+m=2}^{s}\sum_{n=1}^{m-1}[\mathrm{P}^{\cdot}_{m-n(r-r_1-1)}(s-s_1,b-b_1)]_i \times [\mathrm{P}^{\cdot}_{n(r_1-1)}(s_1,b_1)]_i V_i + \sum_{b_1=1}^{b-1}\sum_{s_1+m=2}^{s}k''_{tc}[\mathrm{P}^{\cdot}_{m(r-r_1-1)}(s-s_1-m,b-b)]_i \times [\mathrm{P}^{\cdot}_{0(r_1-1)}(s_1,b_1)]_i V_i \quad i = \mathrm{I},\mathrm{II} \qquad (A.12d)$$

$$T_{4_i} = k'_{fm}[\mathrm{St}]_i[\mathrm{P}^{\cdot}_{0(r)}(s,b)]_i V_i \qquad i = \mathrm{I},\mathrm{II} \qquad (A.12e)$$

where T_1 and T_2 represent the rates of production of PS chains obtained by transfer reactions and by combination termination, respectively; T_3 represents the rate of generation of grafted PS branches by transfer reactions or by combination termination between a primary rubber radical and a PS homoradical or a nonprimary rubber radical; and T_4 represents the rate of generation of grafted PS chains by combination termination between a nonprimary rubber radical and a PS homoradical or another nonprimary rubber radical.

R_p is given by

$$R_p = k_p([\mathrm{S}^{\cdot}] + [\mathrm{P}^{\cdot}])[\mathrm{St}] \qquad (A.13)$$

The dimensionless parameters are defined as follows:

$$\varphi_i = \frac{[\mathrm{S}^{\cdot}]_i}{[\mathrm{S}^{\cdot}]_i + [\mathrm{P}^{\cdot}]_i} \qquad i = \mathrm{I},\mathrm{II} \qquad (A.14)$$

$$\alpha_i = \tau_i + \beta_i \qquad i = \mathrm{I},\mathrm{II} \qquad (A.15)$$

$$\tau_i = \frac{k_{fm}}{k_p} + \frac{k_{fg}[\mathrm{B}^{*}]_i}{(k_p[\mathrm{St}]_i)} + \gamma_i\tau_{1_i} \qquad i = \mathrm{I},\mathrm{II} \qquad (A.16)$$

$$\beta_i = \frac{k_{tc}R_{pi}}{(k_p[\mathrm{St}]_i)^2} \qquad i = \mathrm{I},\mathrm{II} \qquad (A.17)$$

$$\gamma_i = \frac{[\mathrm{P}^{\cdot}_0]_i}{[\mathrm{S}^{\cdot}]_i + [\mathrm{P}^{\cdot}]_i} \qquad i = \mathrm{I},\mathrm{II} \qquad (A.18)$$

$$\tau_{1_i} = \frac{k''_{tc}R_{pi}}{(k_p[\mathrm{St}]_i)^2} \qquad i = \mathrm{I},\mathrm{II} \qquad (A.19)$$

The NCLD of each copolymer topology is obtained by the introduction of eqs. (A.6)–(A.11) and (A.13)–(A.19) into eqs. (A.12); this yields

$$\frac{d}{dt}\{[\mathrm{P}_{(r)}(s,b)]V\} = \sum_i \Bigg\{ -\left[R_{pi}V_i(1-\varphi_i)(\tau_i - \gamma_i\tau_{1_i} + \beta_i\varphi_i + \frac{\gamma_i\tau_{1_i}\varphi_i}{1-\varphi_i})\right]\frac{[\mathrm{B}^*_{(r)}(s,b)]_i}{[\mathrm{B}^*]_i}$$
$$+ [R_{pi}V_i(1-\varphi_i)(\beta_i(1-\varphi_i) + 2\gamma_i\tau_{1_i})] + \left[\frac{R_{pi}^2V_i\gamma_i^2k''_{tc}}{(k_{pi}[\mathrm{St}]_i)^2}\right]$$
$$\times \frac{[\mathrm{B}^*_{(r)}(s,b)]_i}{[\mathrm{B}^*]_i} + R_{pi}V_i(1-\varphi_i)(\tau_i - \gamma_i\tau_{1_i} + \frac{\gamma_i\tau_{1_i}\varphi_i}{1-\varphi_i})$$
$$\times \sum_{m=1}^{s}\frac{[\mathrm{B}^*_{(r-1)}(s-m,b)]_i}{[\mathrm{B}^*]_i}\alpha_i e^{-\alpha_i m} + R_{pi}V_i\varphi_i(1-\varphi_i)\beta_i$$
$$\times \sum_{m=1}^{s}\frac{[\mathrm{B}^*_{(r-1)}(s-m,b)]_i}{[\mathrm{B}^*]_i}\alpha_i^2 m e^{-\alpha_i m} + R_{pi}V_i(1-\varphi_i)\gamma_i\tau_{1_i}$$
$$\times \sum_{b_1=1}^{b-1}\sum_{s_1+m=1}^{s}\frac{[\mathrm{B}^*_{(r-r_1-1)}(s-s_1-m,b-b_1)]_i}{[\mathrm{B}^*]_i} \times \frac{[\mathrm{B}^*_{(r_1-1)}(s_1,b_1)]_i}{[\mathrm{B}^*]_i}\alpha_i e^{-\alpha_i m} + R_{pi}V_i$$
$$\times (1-\varphi_i)^2\frac{\beta_i}{2}\sum_{b_1=1}^{b-1}\sum_{s_1+m=1}^{s}\frac{[\mathrm{B}^*_{(r-r_1-1)}(s-s_1-m,b-b_1)]_i}{[\mathrm{B}^*]_i}$$
$$\times \frac{[\mathrm{B}^*_{(r_1-1)}(s_1,b_1)]_i}{[\mathrm{B}^*]_i}\alpha_i^2 m e^{-\alpha_i m}$$
$$+\frac{R_{pi}^2V_i\gamma_i^2k''_{tc}}{2(k_{pi}[\mathrm{St}]_i)^2}\sum_{b_1=1}^{b-1}\frac{[\mathrm{B}^*_{(r-r_1-1)}(s-s_1,b-b_1)]_i}{[\mathrm{B}^*]_i} \times \frac{[\mathrm{B}^*{}_{r_1-1}(s_1,b_1)]_i}{[\mathrm{B}^*]_i}\Bigg\} \quad r,s,b = 1,2,3,\ldots \quad i = \mathrm{I},\mathrm{II} \qquad (A.20)$$

We obtain the NCLD of the total copolymer, P(*s*,*b*), by adding together eq. (A.20) over all *r* values; this yields

$$\frac{d}{dt}\{[\mathrm{P}(s,b)]V\} = \frac{d}{dt}[\mathrm{P}_{\mathrm{I}}(s,b) + \mathrm{P}_{\mathrm{II}}(s,b)] = \sum_i \Bigg\{ -\left[R_{pi}V_i(1-\varphi_i)(\tau_i - \gamma_i\tau_{1_i} + \beta_i\varphi_i + \frac{\gamma_i\tau_{1_i}\varphi_i}{1-\varphi_i})\right]$$
$$\times \frac{[\mathrm{B}^*(s,b)]_i}{[\mathrm{B}^*]_i} + [R_{pi}V_i(1-\varphi_i)(\beta_i(1-\varphi_i) + 2\gamma_i\tau_{1_i})]$$
$$+ \left[\frac{R_{pi}^2V_i\gamma_i^2k''_{tc}}{(k_p[\mathrm{St}]_i)^2}\right]\frac{[\mathrm{B}^*(s,b)]_i}{[\mathrm{B}^*]_i} + R_{pi}V_i(1-\varphi_i)$$
$$\times (\tau_i - \gamma_i\tau_{1_i} + \frac{\gamma_i\tau_{1_i}\varphi_i}{1-\varphi_i})\sum_{m=1}^{s}\frac{[\mathrm{B}^*(s-m,b)]_i}{[\mathrm{B}^*]_i}\alpha_i e^{-\alpha_i m}$$
$$+ R_{pi}V_i\varphi_i(1-\varphi_i)\beta_i\sum_{m=1}^{s}\frac{[\mathrm{B}^*(S-m,b)]_i}{[\mathrm{B}^*]_i}\alpha_i^2 m e^{-\alpha_i m}$$
$$+ R_{pi}V_i(1-\varphi_i)\gamma_i\tau_{1_i}\sum_{b_1=1}^{b-1}\sum_{s_1+m=1}^{s}\frac{[\mathrm{B}^*(s-s_1-m,b-b_1)]_i}{[\mathrm{B}^*]_i}\frac{[\mathrm{B}^*(s_1,b_1)]_i}{[\mathrm{B}^*]_i}$$
$$\times \alpha_i e^{-\alpha_i m} + R_{pi}V_i(1-\varphi_i)^2\frac{\beta_i}{2}$$
$$\times \sum_{b_1=1}^{b-1}\sum_{s_1+m=1}^{s}\frac{[\mathrm{B}^*(s-s_1-m,b-b_1)]_i}{[\mathrm{B}^*]_i}\frac{[\mathrm{B}^*(s_1,b_1)]_i}{[\mathrm{B}^*]_i}\alpha_i^2 m e^{-\alpha_i m}$$
$$+\frac{R_{pi}^2V_i\gamma_i^2k''_{tc}}{2(k_p[\mathrm{St}]_i)^2}\sum_{b_1=1}^{b-1}\frac{[\mathrm{B}^*(s-s_1,b-b_1)]_i[\mathrm{B}^*(s_1,b_1)]_i}{[\mathrm{B}^*]_i}\frac{}{[\mathrm{B}^*]_i}\Bigg\} \quad s,b = 1,2,3,\ldots \quad i = \mathrm{I},\mathrm{II} \qquad (A.21)$$

Finally, the WCLD of the total GC and the WCLDs of each of its r topologies are obtained by the multiplication of eqs. (A.20) and (A.21) with their corresponding molecular weights (sM_{St} and bM_{Bd}); this yields

$$\begin{aligned}
\frac{d}{dt}G_{GC}(s,b) &= \frac{d}{dt}[G_{GC_I}(s,b) + G_{GC_{II}}(s,b)] = \sum_i \Bigg\{ -[R_{pi}V_i(1-\varphi_i)(\tau_i - \gamma_i\tau_{1_i} + \beta_i\varphi_i + \frac{\gamma_i\tau_{1_i}\varphi_i}{1-\varphi_i})] \\
&\times \frac{[B^*(s,b)]_i}{[B^*]_i}(sM_{St} + bM_{Bd}) + [R_{pi}V_i(1-\varphi_i)(\beta_i(1-\varphi_i) + 2\gamma_i\tau_{1_i})] \\
&+ \left[\frac{R_{pi}^2V_i\gamma_i^2k_{tc}''}{(k_p[St]_i)^2}\right]\frac{[B^*(s,b)]_i}{[B^*]_i}(sM_{St} + bM_{Bd}) + R_{pi}V_i(1-\varphi_i) \\
&\times (\tau_i - \gamma_i\tau_{1_i} + \frac{\gamma_i\tau_{1_i}\varphi_i}{1-\varphi_i})\sum_{m=1}^{s}\frac{[B^*(s-m,b)]_i}{[B^*]_i}\alpha_i e^{-\alpha_i m}(sM_{St} + bM_{Bd}) \\
&+ R_{pi}V_i\varphi_i(1-\varphi_i)\beta_i\sum_{m=1}^{s}\frac{[B^*(s-m,b)]_i}{[B^*]_i}\alpha_i^2 m e^{-\alpha_i m}(sM_{St} + bM_{Bd}) \\
&+ R_{pi}V_i(1-\varphi_i)\gamma_i\tau_{1_i}\sum_{b_1=1}^{b-1}\sum_{s_1+m=1}^{s}\frac{[B^*(s-s_1-m,b-b_1)]_i}{[B^*]_i}\frac{[B^*(s_1,b_1)]_i}{[B^*]_i} \\
&\times \alpha_i e^{-\alpha_i m}(sM_{St} + bM_{Bd}) + R_{pi}V_i(1-\varphi_i)^2\frac{\beta_i}{2} \\
&\times \sum_{b_1=1}^{b-1}\sum_{s_1+m=1}^{s}\frac{[B^*(s-s_1-m,b-b_1)]_i}{[B^*]_i}\frac{[B^*(s_1,b_1)]_i}{[B^*]_i}\alpha_i^2 m e^{-\alpha_i m} \\
&\times (sM_{St} + bM_{Bd}) + \frac{R_{pi}^2V_i\gamma_i^2k_{tc}''}{2(k_p[St]_i)^2}\sum_{b_1=1}^{b-1}\frac{[B^*(s-s_1,b-b_1)]_i}{[B^*]_i} \\
&\times \frac{[B^*(s_1,b_1)]_i}{[B^*]_i}(sM_{St} + bM_{Bd})\Bigg\} \qquad s,b = 1,2,3,\ldots \quad i = I, II
\end{aligned} \tag{A.22}$$

$$\begin{aligned}
\frac{d}{dt}G_{GC_{(r)}}(s,b) &= \frac{d}{dt}[G_{GC_{(r)_I}}(s,b) + G_{GC(r)_{II}}(s,b)] = \sum_i \Bigg\{ -\left[R_{pi}V_i(1-\varphi_i)(\tau_i - \gamma_i\tau_{1_i} + \beta_i\varphi_i + \frac{\gamma_i\tau_{1_i}\varphi_i}{1-\varphi_i})\right] \\
&\times \frac{[B^*_{(r)}(s,b)]_i}{[B^*]_i}(sM_{St} + bM_{Bd}) + [R_{pi}V_i(1-\varphi_i)(\beta_i(1-\varphi_i) + 2\gamma_i\tau_{1_i})] + \left[\frac{R_{pi}^2V_i\gamma_i^2k_{tc}''}{(k_p[St]_i)^2}\right]\frac{[B^*_{(r)}(s,b)]_i}{[B^*]_i}(sM_{St} + bM_{Bd}) \\
&+ R_{Pi}V_i(1-\varphi_i)(\tau_i - \gamma_i\tau_{1_i} + \frac{\gamma_i\tau_{1_i}\varphi_i}{1-\varphi_i})\sum_{m=1}^{s}\frac{[B^*_{(r-1)}(s-m,b)]_i}{[B^*]_i}\times\alpha_i e^{-\alpha_i m}(sM_{St} + bM_{Bd}) + R_{pi}V_i\varphi_i(1-\varphi_i)\beta_i \\
&\times \sum_{m=1}^{s}\frac{[B^*_{(r-1)}(s-m,b)]_i}{[B^*]_i}\alpha_i^2 m e^{-\alpha_i m}(sM_{St} + bM_{Bd}) + R_{pi}V_i(1-\varphi_i)\gamma_i\tau_{1_i}\sum_{b_1=1}^{b-1}\sum_{s_1+m=1}^{s}\frac{[B^*_{(r-r_1-1)}(s-s_1-m,b-b_1)]_i}{[B^*]_i} \\
&\times \frac{[B^*_{(r_1-1)}(s_1,b_1)]_i}{[B^*]_i}\alpha_i e^{-\alpha_i m}(sM_{St} + bM_{Bd}) + R_{pi}V_i(1-\varphi_i)^2\frac{\beta_i}{2}\times\sum_{b_1=1}^{b-1}\sum_{s_1+m=1}^{s}\frac{[B^*_{(r_1-1)}(s-s_1-m,b-b_1)]_i}{[B^*]_i}\frac{[B^*_{(r_1-1)}(s_1,b_1)]_i}{[B^*]_i} \\
&\times \alpha_i^2 m e^{-\alpha_i m}(sM_{St} + bM_{Bd}) + \frac{R_{pi}^2V_i\gamma_i^2k_{tc}''}{2(k_p[St]_i)^2}\times\sum_{b_1=1}^{b-1}\frac{[B^*_{(r-r_1-1)}(s-s_1,b-b_1)]_i}{[B^*]_i}\frac{[B^*_{(r_1-1)}(s_1,b_1)]_i}{[B^*]_i}(sM_{St} + bM_{Bd})\Bigg\} \\
&\qquad s,b = 1,2,3,\ldots \quad i = I, II
\end{aligned} \tag{A.23}$$

The WCLDs of the total free PS and residual PB are

$$\frac{d}{dt}G_{\mathrm{PS}}(n) = \frac{d}{dt}[G_{\mathrm{PS_I}}(n)G_{\mathrm{PS_{II}}}(n)]$$
$$= \sum_i \{[R_{pi}V_i\varphi_i\frac{(\tau_i - \gamma_i\tau_{1_i})}{\alpha_i} + \frac{R_{Pi}V_i\varphi_i^2\beta_i}{2}n]\alpha_i^2 M_{\mathrm{St}}ne^{-\alpha_i n}\}$$
$$n = 1,2,3,\ldots \quad i = \mathrm{I,II} \qquad (A.24)$$

$$\frac{d}{dt}G_{\mathrm{PB}}(b) = \frac{d}{dt}[G_{\mathrm{PB_I}}(b) + G_{\mathrm{PB_{II}}}(b)]$$
$$= \sum_i \Bigg\{ -R_{pi}V_i(1-\varphi_i)(\tau_i - \gamma_i\tau_{1_i} + \beta_i\varphi_i + \frac{\gamma_i\tau_{1_i}\varphi_i}{1-\varphi_i})$$
$$\times \frac{b^2 N_{\mathrm{PB}_i}(b)M_{\mathrm{Bd}}}{[\mathrm{B}^*]_i V_i} - R_{pi}V_i(1-\varphi_i)[\beta_i(1-\varphi_i) + 2\gamma_i\tau_{1_i}]$$
$$\times \frac{b^2 N_{\mathrm{PB}_i}(b)M_{Bd}}{[\mathrm{B}^*]_i V_i} - \frac{R_{pi}^2\gamma_i^2 V_i k'_{tc} b^2 N_{\mathrm{PB}_i}(b)M_{Bd}}{(k_p[\mathrm{St}]_i)^2 \quad [\mathrm{B}^*]_i V_i} \Bigg\}$$
$$b = 1,2,3,\ldots \; i = \mathrm{I,II} \qquad (A.25)$$

After the phase inversion, the free PS accumulates in two PS-rich regions: a particle occlusion region and a continuous phase region. Following Casis et al.,[13] we find that their corresponding MWDs [$G_{\mathrm{PSI,o}}(n)$ and $G_{\mathrm{PSI,c}}(n)$, respectively] are given by

$$\frac{d}{dt}G_{\mathrm{PS_{I,o}}}(n) = \left[\frac{\tau_{\mathrm{I}}}{\alpha_{\mathrm{I}}} + \frac{\beta_{\mathrm{I}}}{2}n\right] R_{P\mathrm{I}}V_{\mathrm{I,o}}\alpha_{\mathrm{I}}^2 M_{\mathrm{St}}ne^{-\alpha_{\mathrm{I}}n}$$
$$+ \left[\frac{(\tau_{\mathrm{II}} - \gamma_{\mathrm{II}}\tau_{1_{\mathrm{II}}})}{\alpha_{\mathrm{II}}} + \frac{\varphi_{\mathrm{II}}\beta_{\mathrm{II}}}{2}n\right] \varphi_{\mathrm{II}}R_{p\mathrm{II}}V_{\mathrm{II}}\alpha_{\mathrm{II}}^2 M_{\mathrm{St}}ne^{-\alpha_{\mathrm{II}}n}$$
$$n = 1,2,3,\ldots \qquad (A.26)$$

$$\frac{d}{dt}G_{\mathrm{PS_{I,c}}}(n) = \left[\frac{\tau_{\mathrm{I}}}{\alpha_1} + \frac{\beta_{\mathrm{I}}}{2}n\right] R_{p\mathrm{I}}V_{\mathrm{I,c}}\alpha_{\mathrm{I}}^2 M_{\mathrm{St}}ne^{-\alpha_{\mathrm{I}}n}$$
$$n = 1,2,3,\ldots \qquad (A.27)$$

Finally, we obtain the expression for the bivariate WCLD of the total HIPS by adding together eqs. (A.22), (A.24), and (A.25) (which is not shown here for reasons of space).

APPENDIX B: MATHEMATICAL MODEL FOR THE UV CHROMATOGRAM OF THE TOTAL HIPS

HIPS is a mixture of free PS, unreacted PB, and GC. Neglecting the UV absorbance by Bd repeating units, we find that the UV chromatogram of the total HIPS [$A_{\mathrm{HIPS}}(V_e)$] is given by

$$A_{\mathrm{HIPS}}(V_e) = A_{\mathrm{PS}}(V_e) + \sum_r A_{\mathrm{GC}_{(r)}}(V_e) \qquad (A.28)$$

where $A_{\mathrm{PS}}(V_e)$ and $A_{\mathrm{GC}_{(r)}}(V_e)$ are the UV chromatograms of the free PS and of the grafted PS branches in each of the GC topologies, respectively. In eq. (A.28), $A_{\mathrm{PS}}(V_e)$ is estimated from the MWD of the free PS, $G_{\mathrm{PS}}(M_{\mathrm{PS}})$ (as predicted by the polymerization model), and the molar mass calibration obtained with PS standards, presented either as $M_{\mathrm{PS}}(V_e)$ or as $\log M_{\mathrm{PS}} = A_1 - B_1V_e$ (Table V); this yields[18]

$$A_{\mathrm{PS}}(V_e) = k_{\mathrm{UV}}M_{\mathrm{PS}}(V_e)G_{\mathrm{PS}}[M_{\mathrm{PS}}(V_e)] \qquad (A.29)$$

where k_{UV} is the gain of the UV spectrophotometer in response to PS mass.

Each of the different GC topologies exhibits a common composition ($\bar{p}_S$), MWDs represented by $G_{\mathrm{GC}_{(r)}}(M)$, and molar mass calibrations represented by $M(V_e,r)$ or, equivalently, by [eq. (5)], for which the parameters A_2, B_2, ε, α_{BC}, and K_{BC} are presented in Table V. Thus, the UV chromatograms of the GC topologies are calculated as follows:

$$A_{\mathrm{GC}}(r)(V_e) = k_{\mathrm{UV}}M(V_e,r)G_{\mathrm{GC}_{(r)}}[M(V_e,r)]\bar{P}_{\mathrm{s}},$$
$$(r = 1,2,\ldots) \qquad (A.30)$$

where the product of $G_{\mathrm{GC}_{(r)}}\bar{p}_S$ represents the instantaneous mass of PS branches eluting at V_e and $M(V_e,r)$ is given by eq. (5). Inserting eqs. (A.29) and (5) into eq. (A.28), we obtain the following expression for the UV chromatogram of the total HIPS:

$$\mathrm{A}_{\mathrm{HIPS}}(V_e) = k_{\mathrm{UV}}$$
$$\times \left\{ M_{\mathrm{PS}}(V_e)G_{\mathrm{PS}}[M_{\mathrm{PS}}(V_e)] + \bar{p}_{\mathrm{s}}\sum_r M(V_e)G_{\mathrm{GC}}[M(V_e,r)] \right\} \qquad (A.32)$$

Note that the areas under $A_{\mathrm{PS}}(V_e)$ and $A_{\mathrm{HIPS}}(V_e)$ are proportional to the masses of free PS and totally polymerized St, respectively. Also, note that the units of $A_{\mathrm{HIPS}}(V_e)$ are arbitrary, and so k_{UV} is not strictly required.

NOMENCLATURE

A_1, B_1 and A_2, B_2	y intercepts and slopes of the (linear) direct and universal molecular weight calibrations
$A_{\mathrm{DR}}(V_e)$ and $A_{\mathrm{SV}}(V_e)$	concentration chromatogram obtained from a differential refractometer and specific viscosity chromatogram
$A_{\mathrm{GC}_{(r)}}(V_e)$, $A_{\mathrm{HIPS}}(V_e)$, and $A_{\mathrm{PS}}(V_e)$	UV chromatograms of the free PS, grafted PS branches, and total HIPS
b	number of Bd repetitive units
B*	nongrafted Bd repetitive unit
$\mathrm{B}^*_{(r)}(s,b)$	nongrafted Bd unit of $\mathrm{P}_{(r)}(s,b)$
Bd	butadiene
BPO	n-butyl peroctoate
E_{St}	St grafting efficiency
E_{PB}	PB grafting efficiency
f	initiator efficiency

g' and g	branching contraction parameters [defined by eqs. (1) and (3)]
G	mass (g)
$G_{PS}(M)$, $G_{GC}(M)$, $G_{GC_{(r)}}(M)$, and $G_{PB}(M)$	molecular weight distributions of the free PS, GC, a generic rth copolymer topology, and residual PB
GC	graft copolymer
HIPS	high-impact polystyrene
$I^{\cdot}$	primary initiator radical
I_2	chemical initiator
k_d	initiator decomposition rate constant
k_{fg}	rate constant of chain transfer to the rubber
k_{i1}, k_{i2}, and k_{p0}	initiation rate constants
k_{i3}	rate constant of thermal monomer initiation
k_p	propagation rate constant
k_{tc} and k_{tc}''	rate constants of termination by recombination
K	Mark–Houwink factor
K_{I_2}	initiator partition coefficient
k_{UV}	UV sensor gain
M	molar mass
M_{Bd} and M_{St}	molecular weights of Bd and St repeating units
M_n	number-average molecular weight
M_w	weight-average molecular weight
MWD	molecular weight distribution
$M(V_e)$	molecular weight calibration in SEC
NCLD	number chain length distribution
$\overline{p}_S$	global St mass fraction in the GC
$P^{\cdot}$	generic GC radical with a growing polystyryl chain
$P^{\cdot}_0$	generic primary rubber radical
$P^{\cdot}_{0(r)}(s,b)$	primary rubber radical of topology r and chain lengths s and b
$P^{\cdot}_{n(r)}(s,b)$	radical species produced from $P^{\cdot}_{0(r)}(s,b)$, containing a new growing PS chain with n repetitive units
$P_{(r)}(s,b)$	GC molecule of topology r with s repetitive units of St and b repetitive units of Bd (includes unreacted PB with $r = s = 0$)
PB	polybutadiene
PS	polystyrene
r	number of trifunctional grafting points per GC molecule
R_p	global rate of St consumption
R_{pPS_I} and $R_{pPS_{II}}$	generation rates of free PS in phases I and II (mol/L s^{-1})
s	number of St repetitive units
$\langle s^2 \rangle$	average square radius of gyration
$S^{\cdot}$	primary St radical
S_n	PS molecule of chain length n
$S^{\cdot}_n$	polystyryl homoradical of chain length n
SEC	size exclusion chromatography
St	styrene
t	time (s)
T	temperature (°C)
T_1 and T_2	rates of production of PS chains obtained by transfer reactions and by combination termination
T_3	rate of generation of grafted PS branches by transfer reactions or by combination termination between a primary rubber radical with a PS homoradical or with a nonprimary rubber radical
T_4	rate of generation of grafted PS chains by combination termination between a nonprimary rubber radical with a PS homoradical or with another nonprimary rubber radical
TBPO	*tert*-butyl peroctoate
UV	ultraviolet
V	reaction volume (L)
V_e	elution volume (mL)
WCLD	weight chain length distribution

Greek symbols

α	Mark–Houwink exponent
β, φ, γ, θ, τ, and τ_1	dimensionless kinetic parameters
ε	exponent defined by eq. (2)
$[\eta]$	intrinsic viscosity
ψ_i	polymer volume fraction in phase i

Subscripts

b	branched molecule
(c)	continuous region of the PS-rich phase
I and II	PS-rich phase and PB-rich phase
l	linear molecule
(o)	particle occlusion region of the PS-rich phase

References

1. Fischer, M.; Hellmann, G. P. Macromolecules 1996, 29, 2498.
2. Choi, J. H.; Ahn, K. H.; Kim, S. Y. Polymer 2000, 41, 5229.
3. Okamato, Y.; Miyagi, H.; Kakugo, M.; Takahashi, K. Macromolecules 1991, 24, 5639.
4. Katime, I.; Quintana, J. R.; Price, C. Mater Lett 1995, 22, 297.
5. Sudduth, R. D. J Appl Polym Sci 1978, 22, 2427.

6. Ludwico, W. A.; Rosen, S. L. J Appl Polym Sci 1975, 19, 757.
7. Ludwico, W. A.; Rosen, S. L. J Appl Polym Sci 1976, 14, 2121.
8. Schierholz, J. U.; Hellmann, G. P. Polymer 2003, 44, 2005.
9. Soto, G.; Nava, E.; Rosas, M.; Fuenmayor, M.; González, I.; Meira, G.; Oliva, H. J Appl Polym Sci 2003, 92, 1397.
10. García, N.; Meira, G.; Oliva, H. Simp Latinoam Polím 2002, 8, 321.
11. Berlin, D.; Couland, F.; Duc, M.; Galindo, C.; Gigmes, D.; Marque, S.; Tordo, P.; Vuillemin, B. Polymers 2004, 10.
12. Estenoz, D. A.; Gonzalez, I. M.; Oliva, H. M.; Meira, G. R. J Appl Polym Sci 1999, 74, 1950.
13. Casis, N.; Estenoz, D. A.; Oliva, H. M.; Meira, G. R. J Appl Polym Sci 2006, 99, 3023.
14. Estenoz, D. A.; Vega, J. R.; Oliva, H. M.; Meira, G. R. Int J Polym Anal Char 2001, 6, 315.
15. Estenoz, D. A.; Vega, J. R.; Oliva, H. M.; Meira, G. R. J Liq Chromatogr Relat Technol 2002, 25, 2781.
16. Zimm, B. H.; Stockmayer, W. H. J Chem Phys 1949, 17, 1301.
17. Vega, J. R.; Estenoz, D. A.; Oliva, H. M.; Meira, G. R. Int J Polym Anal Char 2001, 6, 339.
18. Meira, G. R.; Vega, J. R.; Yossen, M. M. In Ewing's Analytical Instrumentation Handbook, 3rd ed.; Cazes, J., Ed.; Marcel Dekker: New York, 2004; p 825.